

Small-Scale Structure of Spacetime: Bounds and Conjectures

F.R. Klinkhamer

Institute for Theoretical Physics, University of Karlsruhe (TH), 76128 Karlsruhe, Germany

Abstract. This review consists of two parts. The first part establishes certain astrophysical bounds on the smoothness of classical spacetime. Some of the best bounds to date are based on the absence of vacuum Cherenkov radiation in ultrahigh-energy cosmic rays. The second part discusses possible implications of these bounds for the quantum structure of spacetime. One conjecture is that the fundamental length scale of quantum spacetime may be different from the Planck length.

Keywords: spacetime topology, quantum gravity, Lorentz violation, vacuum Cherenkov radiation

PACS: 04.20.Gz, 04.60.-m, 11.30.Cp, 41.60.Bq

1. INTRODUCTION

The present contribution addresses the following basic question: *does space remain smooth as one probes smaller and smaller distances?* A conservative limit on the typical length scale ℓ of any nontrivial small-scale structure of space results from the fact that the experimental data from particle accelerators such as LEP at CERN and the Tevatron at Fermilab are perfectly well described by relativistic quantum fields over a smooth manifold (specifically, Minkowski spacetime),

$$\ell|_{\text{LEP/Tevatron}} \lesssim 10^{-18} \text{ m} \approx \hbar c / (200 \text{ GeV}) . \quad (1)$$

Remark that the last approximate equality in (1) follows from the Heisenberg uncertainty principle applied to the matter probes, even though the bounded spacetime length ℓ itself may be a purely classical quantity.

Yet, astrophysics provides us with very much higher energies to probe spacetime. A possible strategy is then

- to consider the phenomenology of simple spacetime models;
- to obtain bounds on the model parameters from ultrahigh-energy cosmic rays;
- to establish the main theoretical implications.

Some of our recent work has pursued the above strategy and the aim of the present article is to review this work in a coherent fashion. In Sec. 2, we discuss the phenomenology of two simple models for modified photon propagation [1, 2]. In Secs. 3.1 and 3.2, we obtain ultrahigh-energy cosmic-ray (UHECR) bounds [1, 2, 3] on the parameters of the two types of models considered and, in Sec. 3.3, we discuss some implications. In Sec. 4, which can be read independently of Secs. 2 and 3, we put forward two conjectures [4] on the fundamental length of a hypothetical small-scale structure of quantum spacetime. In Sec. 5, we summarize our results.

2. PHENOMENOLOGY

Two simple models of photon propagation will be presented in this section. The first model has the standard quadratic Maxwell action density term integrated over a flat spacetime manifold with “defects.” For this first model, the modified photon dispersion relation will be calculated in the long-wavelength approximation.

The second model has a quadratic modified-Maxwell term integrated over standard Minkowski spacetime. The corresponding photon dispersion relation can be readily obtained. Having standard Dirac fermions coupled to photons with modified propagation properties, the process of “vacuum Cherenkov radiation” may be allowed for certain combinations of Lorentz-violating parameters. For the second model, the relevant Cherenkov energy threshold will be given explicitly.

2.1. Model 1

Consider standard Quantum Electrodynamics (QED) [5] over a classical spacetime-foam¹ manifold (with details to be specified later), which has the following action:

$$S_{\text{Model 1}} = \int'_{\text{foam}} d^4x \left(-\frac{1}{4} \eta^{\mu\rho} \eta^{\nu\sigma} F_{\mu\nu}(x) F_{\rho\sigma}(x) + \bar{\psi}(x) \left(\gamma^\mu (i \partial_\mu - e A_\mu(x)) - M \right) \psi(x) \right), \quad (2)$$

where $F_{\mu\nu}(x) \equiv \partial_\mu A_\nu(x) - \partial_\nu A_\mu(x)$ is the Maxwell field strength tensor of the gauge field $A_\mu(x)$ and $\psi(x)$ the Dirac spinor field corresponding to, e.g., a proton with electric charge e and rest mass M .

The prime on the integral sign of (2) indicates the restriction to the flat Minkowski part of the manifold with specific boundary conditions at certain submanifolds called “defects.” The procedure can perhaps best be illustrated by the example of Fig. 1 on the next page, where the static “wormholes” [6, 7] are sliced off (or, more accurately, the wormhole “throats” are taken to have zero lengths) and the resulting holes/defects in flat spacetime are given appropriate boundary conditions for the vector and spinor fields appearing in (2); see Fig. 2 for a sketch.

The coordinates of flat spacetime are denoted by $(x^\mu) = (x^0, \mathbf{x}) = (ct, x^1, x^2, x^3)$ and the standard Minkowski metric is $(\eta_{\mu\nu}) = \text{diag}(1, -1, -1, -1)$. The Levi-Civita symbol $\epsilon_{\mu\nu\rho\sigma}$, which will be used later, is normalized by $\epsilon_{0123} = 1$. The direction of a 3-vector \mathbf{x} is given by the unit 3-vector $\hat{\mathbf{x}} \equiv \mathbf{x}/|\mathbf{x}|$. In this section and the next, we use natural units with $c = \hbar = 1$, but, occasionally, we display c or \hbar in order to clarify the physical dimensions of a particular expression. The dimensionful constants c and \hbar will, however, occupy the center of the stage in Sec. 4.

¹ A note of caution may be in order, as the terminology “spacetime foam” is often considered to refer solely to the quantum structure of spacetime [6, 7, 8, 9], whereas, here, the picturesque designation “classical spacetime-foam manifold” simply refers to a classical manifold with nontrivial small-scale structure (resembling, for example, a well-known Swiss cheese). The elusive “quantum structure of spacetime” will be discussed further in Sec. 4, whereas we remain with the more or less familiar classical spacetime in Secs. 2 and 3.

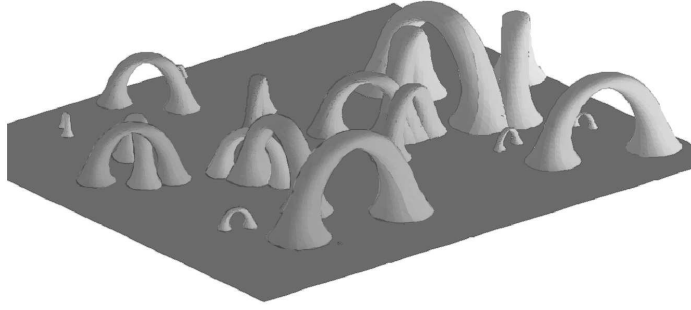


FIGURE 1. Example of a static (time-independent) classical spacetime foam, with one spatial dimension suppressed. The corresponding spacetime is mostly flat (Minkowski-like) and has several permanent wormholes added.

Next, take some very simple classical spacetime-foam models with:

- identical defects (spacetime size \bar{b}) embedded in Minkowski spacetime,
- a homogeneous and isotropic distribution of defects (spacetime density $n \equiv 1/\bar{l}^4$),
- a strong dilution of defects ($\bar{b} \ll \bar{l}$),

where the last requirement, in particular, is a purely technical assumption in order to simplify the calculation.

Remark that, for the classical spacetime shown in Fig. 1, there is no topology change (in fact, it is unclear whether or not topology change is allowed at all; see, e.g., Ref. [9]). As far as our calculations are concerned, the detailed dynamics of the classical defects considered does not appear to be important; what matters are average quantities such as the typical defect size and separation.

Now calculate the proton and photon dispersion relations in the long-wavelength approximation, $\lambda \gg \bar{l} \gg \bar{b}$. No details of the calculation [1] will be given here but only the heuristics for the photon case: *localized defects correspond to fictional multipoles* which affect the propagation of electromagnetic plane waves. Electromagnetic-wave

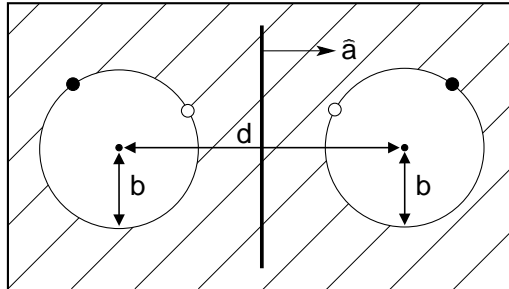


FIGURE 2. Three-space from a single wormhole-like defect (two spheres with equal radius b and distance $d > 2b$ between their centers) embedded in \mathbb{R}^3 , with the “interiors” of the two spheres removed and their points identified by reflection in a central plane with normal unit vector $\hat{\mathbf{a}}$. If the “long distance” d between the centers of the wormhole mouths is of the same order of magnitude as their width $2b$, the defect is effectively localized in the ambient three-space.

propagation over a spacetime with defects is then different from propagation over a perfectly smooth Minkowski spacetime. In fact, the basic physics is the same as that of the so-called “Bethe holes” in waveguides [10]. It is clear that different types of localized defects give essentially the same result, just with different numerical coefficients.

The modified proton (p) and photon (γ) dispersion relations for wave number $k \equiv |\mathbf{k}| \equiv 2\pi/\lambda$ can, therefore, be given in completely general form (that is, independent of the detailed calculations):

$$\omega_p^2 \equiv \tilde{m}_p^2 c_p^4 / \hbar^2 + c_p^2 k^2 + \mathcal{O}(c_p^2 \tilde{b}^2 k^4), \quad (3a)$$

$$\omega_\gamma^2 = (1 + \tilde{\sigma}_2 \tilde{F}) c_p^2 k^2 + \tilde{\sigma}_4 \tilde{F} c_p^2 \tilde{b}^2 k^4 + \mathcal{O}(c_p^2 \tilde{b}^4 k^6), \quad (3b)$$

with c_p^2 simply defined as the coefficient of the quadratic proton term, effective on/off factors $\tilde{\sigma}_2, \tilde{\sigma}_4 \in \{-1, 0, +1\}$, an effective defect size \tilde{b} , and an effective excluded-volume factor

$$\tilde{F} \equiv (\tilde{b}/\tilde{l})^4, \quad (4)$$

which, for the moment, is assumed to be much less than unity.

Observe that the calculated dispersion relations as given by (3ab) do not contain cubic terms in k , consistent with general arguments based on coordinate independence and rotational invariance [11]. Furthermore, the photon dispersion relations found are the same for both polarization modes (absence of birefringence) because of the assumed isotropy of the defect distributions. However, the photon dispersion relations do show birefringence, but still no cubic terms, if there is assumed to be an anisotropic distribution of intrinsically asymmetric defects (having, for example, defects from Fig. 2 with all axes $\hat{\mathbf{a}}$ aligned).

As mentioned above, calculations of certain simple spacetime-foam models give the effective dispersion-relation parameters (with tildes) in terms of the underlying spacetime parameters (with bars):

$$\tilde{b} = \beta \bar{b}, \quad \tilde{l} = \chi \bar{l}, \quad \tilde{\sigma}_2 = -1, \quad \tilde{\sigma}_4 = 1, \quad (5)$$

where β and χ are positive numerical constants of order unity, which depend on the details of the defects considered. Note that, for static defects as in Fig. 2, with size b and separation l , a physically more appropriate definition of \tilde{F} would be $(b/l)^3$, but, mathematically, definition (4) with $(b/l)^4$ can still be used.

With intrinsically different boundary conditions at the defect locations for the different types of matter fields (spinor and vector), the quadratic terms of the proton and photon dispersion relations can be expected to be different in general. Having defined the quadratic proton term in (3a) as $c_p^2 k^2$, the quadratic photon term in (3b) will then differ from $c_p^2 k^2$, unless the defects are infinitely small or infinitely far apart. The resulting unequal proton and photon velocities may lead to new types of decay processes [12], for example, vacuum Cherenkov radiation $p \rightarrow p \gamma$ for the case of a negative coefficient $\tilde{\sigma}_2 \tilde{F}$ in (3b). This particular decay process will be discussed further in the next subsection.

Regardless of the origin and interpretation, it is clearly important to obtain bounds on the effective parameters \tilde{F} and \tilde{b} in the modified photon dispersion relation (3b) for a proton dispersion relation given by (3a).

2.2. Model 2

In the previous subsection, we have found a quadratic photon term of the dispersion relation which was modified by a single parameter \tilde{F} determined by the underlying structure of spacetime. This type of modified photon propagation can easily be generalized.

Consider the following action for a Lorentz-violating deformation of QED:

$$S_{\text{Model 2}} = S_{\text{modM}} + S_{\text{standD}}, \quad (6)$$

with a modified-Maxwell term [13, 14],

$$S_{\text{modM}} = \int_{\mathbb{R}^4} d^4x \left(-\frac{1}{4} (\eta^{\mu\rho} \eta^{\nu\sigma} + \kappa^{\mu\nu\rho\sigma}) F_{\mu\nu}(x) F_{\rho\sigma}(x) \right), \quad (7)$$

and the standard Dirac term [5] for a spin- $\frac{1}{2}$ particle with charge e and mass M ,

$$S_{\text{standD}} = \int_{\mathbb{R}^4} d^4x \bar{\psi}(x) \left(\gamma^\mu (i \partial_\mu - e A_\mu(x)) - M \right) \psi(x). \quad (8)$$

Theory (6) is gauge-invariant, CPT-even, and power-counting renormalizable.

The quantity $\kappa^{\mu\nu\rho\sigma}$ in the modified-Maxwell term (7) is a constant background tensor with real and dimensionless components. This background tensor $\kappa^{\mu\nu\rho\sigma}$ has, in fact, the same symmetries as the Riemann curvature tensor and a double trace condition $\kappa^{\mu\nu}_{\mu\nu} = 0$, so that there are $20 - 1 = 19$ independent components. All components of the κ -tensor in (7) are assumed to be sufficiently small in order to ensure energy positivity.

As the ten birefringent parameters are already constrained at the 10^{-32} level [15], restrict the theory to the nonbirefringent sector by making the following *Ansatz* [16]:

$$\kappa^{\mu\nu\rho\sigma} = \frac{1}{2} (\eta^{\mu\rho} \tilde{\kappa}^{\nu\sigma} - \eta^{\nu\rho} \tilde{\kappa}^{\mu\sigma} + \eta^{\nu\sigma} \tilde{\kappa}^{\mu\rho} - \eta^{\mu\sigma} \tilde{\kappa}^{\nu\rho}), \quad (9)$$

for a symmetric and traceless matrix $\tilde{\kappa}^{\mu\nu}$ with $10 - 1 = 9$ independent components. Rewrite these nine Lorentz-violating “deformation parameters” $\tilde{\kappa}^{\mu\nu}$ as follows:

$$(\tilde{\kappa}^{\mu\nu}) \equiv \text{diag}(1, \frac{1}{3}, \frac{1}{3}, \frac{1}{3}) \bar{\kappa}^{00} + (\delta \tilde{\kappa}^{\mu\nu}), \quad \delta \tilde{\kappa}^{00} = 0, \quad (10)$$

with one independent parameter $\bar{\kappa}^{00}$ for the spatially isotropic part of $\tilde{\kappa}^{\mu\nu}$ and eight independent parameters $\delta \tilde{\kappa}^{\mu\nu}$ which need not be smaller than $\bar{\kappa}^{00}$.

For later use, also define a vector $\vec{\alpha}$ in parameter space \mathbb{R}^9 :

$$\vec{\alpha} \equiv \begin{pmatrix} \alpha^0 \\ \alpha^1 \\ \alpha^2 \\ \alpha^3 \\ \alpha^4 \\ \alpha^5 \\ \alpha^6 \\ \alpha^7 \\ \alpha^8 \end{pmatrix} \equiv \begin{pmatrix} \tilde{\alpha}^{00} \\ \tilde{\alpha}^{01} \\ \tilde{\alpha}^{02} \\ \tilde{\alpha}^{03} \\ \tilde{\alpha}^{11} \\ \tilde{\alpha}^{12} \\ \tilde{\alpha}^{13} \\ \tilde{\alpha}^{22} \\ \tilde{\alpha}^{23} \end{pmatrix} \equiv \begin{pmatrix} (4/3) \bar{\kappa}^{00} \\ 2 \delta \tilde{\kappa}^{01} \\ 2 \delta \tilde{\kappa}^{02} \\ 2 \delta \tilde{\kappa}^{03} \\ \delta \tilde{\kappa}^{11} \\ \delta \tilde{\kappa}^{12} \\ \delta \tilde{\kappa}^{13} \\ \delta \tilde{\kappa}^{22} \\ \delta \tilde{\kappa}^{23} \end{pmatrix}, \quad (11)$$

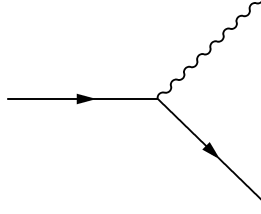


FIGURE 3. Feynman diagram for vacuum Cherenkov radiation.

which is taken to have the standard Euclidean norm,

$$|\vec{\alpha}|^2 \equiv \sum_{l=0}^8 (\alpha^l)^2. \quad (12)$$

Note that the negative of the isotropic parameter α^0 corresponds, in leading order, to the coefficient $\tilde{\sigma}_2 \tilde{F}$ of the modified photon dispersion relation (3b) calculated for Model 1.

It may be of interest to mention that, whereas Model 2 has constant deformation parameters (9), another model has a small stochastic parameter $g(x)$ multiplying a CPT-odd action density term $\varepsilon^{\mu\nu\rho\sigma} F_{\mu\nu}(x) F_{\rho\sigma}(x)$. This particular stochastic model has been studied in the long-wavelength approximation in Ref. [17]. Recently, we have become aware of a complementary paper [18], which considers similar models in the short-wavelength approximation.

Model 2 has, for appropriate deformation parameters $\vec{\alpha}$, a maximum proton velocity larger than the phase velocity of light, which allows for vacuum Cherenkov radiation $p \rightarrow p\gamma$. This particular decay process has been studied classically by Altschul [19] and quantum-mechanically at tree-level (Fig. 3) by Kaufhold and the present author [2, 12]. The radiated-energy rate of a primary (on-shell) particle with point charge $Z_{\text{prim}} e$, mass $M_{\text{prim}} > 0$, momentum \mathbf{q}_{prim} , and ultrarelativistic energy $E_{\text{prim}} \sim c |\mathbf{q}_{\text{prim}}|$ is asymptotically given by [2]

$$\left. \frac{dW_{\text{Model 2}}(\hat{\mathbf{q}}_{\text{prim}}, E_{\text{prim}})}{dt} \right|_{E_{\text{prim}}^2 \gg E_{\text{thresh}}^2} \sim Z_{\text{prim}}^2 \frac{e^2}{4\pi} \xi(\hat{\mathbf{q}}_{\text{prim}}) E_{\text{prim}}^2 / \hbar, \quad (13)$$

with a nonnegative dimensionless coefficient $\xi(\hat{\mathbf{q}}_{\text{prim}})$ from appropriate contractions of the κ -tensor with two rescaled q -vectors and the squared threshold energy [19]

$$E_{\text{thresh}}^2 = \frac{M_{\text{prim}}^2 c^4}{R_\varepsilon(\alpha^0 + \alpha^j \hat{\mathbf{q}}_{\text{prim}}^j + \tilde{\alpha}^{jk} \hat{\mathbf{q}}_{\text{prim}}^j \hat{\mathbf{q}}_{\text{prim}}^k)} + \mathcal{O}(M_{\text{prim}}^2 c^4), \quad (14)$$

in terms of a regularized ramp function $R_\varepsilon(x) \equiv \varepsilon + (x + |x|)/2$ for a real variable x and an arbitrarily small positive parameter ε .

Exact tree-level results have been obtained recently [20] for the restricted model (labeled “isotropic case”) with $\alpha_0 \equiv \alpha^0 > 0$ and $\alpha^l = 0$, for $l = 1, \dots, 8$. Setting again $\hbar = c = 1$, the radiated-energy rate for a spin- $\frac{1}{2}$ Dirac particle (charge e , mass M , and

energy E above threshold) is given by the following expression:

$$\begin{aligned} \frac{dW_{\text{Model2}}^{\text{isotropic case}}}{dt} &= \frac{e^2}{4\pi} \frac{1}{3\alpha_0^3 E \sqrt{E^2 - M^2}} \left(\sqrt{\frac{2 - \alpha_0}{2 + \alpha_0}} E - \sqrt{E^2 - M^2} \right)^2 \\ &\times \left\{ 2(\alpha_0^2 + 4\alpha_0 + 6) E^2 - (2 + \alpha_0) \right. \\ &\times \left. \left(3(1 + \alpha_0) M^2 + 2(3 + 2\alpha_0) \sqrt{\frac{2 - \alpha_0}{2 + \alpha_0}} E \sqrt{E^2 - M^2} \right) \right\}. \quad (15) \end{aligned}$$

The high-energy expansion of (15) for fixed parameters α_0 and M reads

$$\begin{aligned} \frac{dW_{\text{Model2}}^{\text{isotropic case}}}{dt} &= \frac{e^2}{4\pi} \left\{ \left(\frac{7}{24} \alpha_0 - \frac{1}{16} \alpha_0^2 + O(\alpha_0^3) \right) E^2 \right. \\ &\quad \left. + \left(-1 + \frac{1}{48} \alpha_0 - \frac{3}{32} \alpha_0^2 + O(\alpha_0^3) \right) M^2 + O\left(\frac{M^4}{\alpha_0 E^2} \right) \right\}, \quad (16) \end{aligned}$$

which shows the quadratic behavior of (13) with factor $Z_{\text{prim}}^2 = 1$ and constant coefficient $\xi = (7/24) \alpha_0$. From (15), one also obtains the exact threshold energy (temporarily reinstating c):

$$E_{\text{thresh}}^{\text{Model2, isotropic case}} = \frac{Mc^2}{\sqrt{\alpha_0}} \sqrt{1 + \alpha_0/2}, \quad (17)$$

which reproduces (14) for $M = M_{\text{prim}}$ and small enough positive $\alpha_0 \equiv \alpha^0$. Incidentally, the numerical value of α_0 cannot be too large, as the factors $\sqrt{2 - \alpha_0}$ in (15) make clear.

Returning to Model 2 with generic deformation parameters α^l , it is to be expected that vacuum Cherenkov radiation only occurs for those parameters $\vec{\alpha}$ for which the phase velocity of light is less than the maximal attainable velocity c of the charged particle in theory (6), $v_{\text{ph}} < c$. In fact, this phase-velocity condition corresponds to having a positive argument of the ramp function on the right-hand side of (14). The relevant domain in parameter space is given by

$$D_{\text{causal}}^{(\text{open})} \equiv \{ \vec{\alpha} \in \mathbb{R}^9 : \forall_{\hat{\mathbf{x}} \in \mathbb{R}^3} (\alpha^0 + \alpha^j \hat{x}^j + \tilde{\alpha}^{jk} \hat{x}^j \hat{x}^k) > 0 \}, \quad (18)$$

for arbitrary unit 3-vector $\hat{\mathbf{x}} \equiv \mathbf{x}/|\mathbf{x}|$. The superscript ‘(open)’ in (18) refers to the use of the open relation symbol ‘>’ on the right-hand side instead of the closed symbol ‘≥’, because there is no vacuum Cherenkov radiation for the case of $v_{\text{ph}} = c$. Most likely, the domain (18) constitutes a significant part of the physical domain of theory (6), where, e.g., microcausality holds. Hence, the subscript ‘causal’ in (18).

Microcausality of Lorentz-violating theories has been discussed in, for example, Refs. [21, 22, 23]. To this author, it is clear that violation of microcausality is unacceptable in the type of theories considered here, because, for a spacelike separation of two events, the time order can be interchanged by an appropriate observer Lorentz

transformation. Perhaps not unacceptable (at least, according to our current experimental knowledge) is a new class of particle instabilities which occur at ultralarge three-momentum due to energy non-positivity (at least, in “concordant” frames, where the Lorentz-violating parameters are relatively small).

Let us end this subsection with a general remark on Model 2 (see also Sec. 3.3 for further discussion). New phenomena at the energy scale $E_{\text{Planck}} \approx 10^{19}$ GeV [6, 7] may lead to Lorentz violation in the low-energy theory, partially described by the model action (6). But the resulting Lorentz-violating parameters $\vec{\alpha}$ need not be extremely small (e.g., suppressed by inverse powers of E_{Planck}) and can be of order unity, as long as the theory remains physically consistent. In fact, the modified-dispersion-relation calculations from the previous subsection provide an example: the quadratic coefficient \tilde{F} in (3b) can, in principle, be close to one. Hence, it is important to obtain as strong bounds as possible on *all* deformation parameters $\vec{\alpha}$.

3. UHECR CHERENKOV BOUNDS

The goal of this section is to establish bounds on the parameters of the two Lorentz-violating models discussed in the previous section. One type of bounds relies on the process of vacuum Cherenkov radiation (Fig. 3) already mentioned in Sec. 2.2.

The basic idea is simple [24, 25]:

- if vacuum Cherenkov radiation has a threshold energy $E_{\text{thresh}}(\tilde{b}, \tilde{l}, \vec{\alpha})$ and the radiation rate above threshold is not suppressed, then UHECRs with $E_{\text{prim}} > E_{\text{thresh}}$ cannot travel far (certainly not over distances of the order of megaparsecs), as they rapidly radiate away their energy;
- observing an UHECR then implies a primary energy E_{prim} at or below threshold, which gives bounds on combinations of \tilde{b} , \tilde{l} , and $\vec{\alpha}$.

Expanding on the last point, the following inequality must hold for the *measured* primary energy E_{prim} of an UHECR compared to the *theoretical* result for the threshold energy:

$$E_{\text{prim}} \leq E_{\text{thresh}}(\tilde{b}, \tilde{l}, \vec{\alpha}), \quad (19)$$

which can be written as an upper bound on the parameters of the Lorentz-violating theory considered (here, taken to be \tilde{b} , \tilde{l} , and $\vec{\alpha}$, from the two models discussed in the two previous subsections).

Incidentally, other types of bounds [1] have been obtained (specifically, from the lack of time dispersion and Rayleigh-like scattering in a particular TeV gamma-ray flare from the active galaxy Mkn 421), but the resulting bounds are, for the moment, less tight than those from the inferred absence of vacuum Cherenkov radiation.

3.1. UHECR Bounds – Model 1

In order to obtain Cherenkov bounds [1] for the two parameters \tilde{b} and \tilde{l} of Model 1, start with the spectacular event [26] shown in Fig. 4 a few pages later. This particular

Extensive Air Shower (EAS) event corresponds, in fact, to the most energetic particle observed to date, having an energy $E_{\text{prim}} \approx 300 \text{ EeV} = 3 \times 10^{11} \text{ GeV} = 3 \times 10^{20} \text{ eV}$.

From the EAS event of Fig. 4, we obtain the following Cherenkov-like bounds on the quadratic and quartic coefficients of dispersion relation (3b):

$$-3 \times 10^{-23} \lesssim \tilde{\sigma}_2 \tilde{F} \lesssim 3 \times 10^{-23}, \quad (20a)$$

$$-(7 \times 10^{-39} \text{ m})^2 \lesssim \tilde{\sigma}_4 \tilde{F} \tilde{b}^2 \lesssim (5 \times 10^{-38} \text{ m})^2, \quad (20b)$$

based on the detailed analysis of Ref. [27] (some back-of-the-envelope calculations have been presented in App. B of Ref. [28]). For bounds (20ab), the primary was assumed to be a proton (p) with standard partonic distributions and, as mentioned before, its energy was determined to be $E_p \approx 3 \times 10^{11} \text{ GeV}$.

Note that the above bounds are two-sided, whereas genuine Cherenkov radiation would only give one-sided bounds (the electromagnetic-wave phase velocity must be less than the maximum particle velocity). The reason for having two-sided bounds is that, in addition to Cherenkov radiation, another type of process can occur, namely, proton break-up $p \rightarrow p e^+ e^-$ (pair-production by a virtual gauge boson), which gives the “other” sides of the bounds [27].

It is important to understand the dependence of bounds (20ab) on the assumed primary mass (here, taken as $M_{\text{prim}} = 0.94 \text{ GeV}/c^2$) and primary energy (here, taken as $E_{\text{prim}} = 3 \times 10^{11} \text{ GeV}$). The high and low limits of bounds (20a) and (20b) are multiplied by scaling factors $f_{a,\text{high/low}}$ and $f_{b,\text{high/low}}$, respectively, which are approximately given by

$$f_{a,\text{high}} \approx f_{a,\text{low}} \approx (M_{\text{prim}} c^2 / 0.94 \text{ GeV})^2 (3 \times 10^{11} \text{ GeV} / E_{\text{prim}})^2, \quad (21a)$$

$$f_{b,\text{high}} \approx f_{b,\text{low}} \approx (M_{\text{prim}} c^2 / 0.94 \text{ GeV})^2 (3 \times 10^{11} \text{ GeV} / E_{\text{prim}})^4. \quad (21b)$$

Bounds (20ab) would certainly be less compelling if the Fly’s Eye event of Fig. 4 were unique. But, luckily, this is not the case, as the Pierre Auger Observatory [29] has already seen an event (ID No. 737165) with a similar energy of $2 \times 10^{11} \text{ GeV}$ [30].

Let us end this subsection with a somewhat peripheral remark. The extremely small numbers of order $10^{-38} \text{ m} \approx \hbar c / (2 \times 10^{22} \text{ GeV})$ appearing in the Cherenkov-like bound (20b), which traces back to Eq. (1.14) of Ref. [27], appear to be incompatible with a quartic-term mass scale $M_{\text{QG2}} \approx 6 \times 10^{10} \text{ GeV}$ claimed [31] to be a possible explanation of time-dispersion effects observed in the July 9, 2005 gamma-ray flare from Mkn 501 by the MAGIC telescope (see, in particular, Fig. 7 of Ref. [32]). Even though we have doubts as to the validity of this possible detection of “quantum-gravity” effects,² it is instructive to see how, in principle, astrophysical data could give more than just bounds on the possible small-scale structure of space.

² Note also that the June 30, 2005 flare, for the two medium-energy bands 0.25 – 0.60 TeV and 0.60 – 1.20 TeV shown in Fig. 6 of Ref. [32], appears to have a time-dispersion behavior *opposite* to that of the July 9, 2005 flare, as shown in Fig. 7 of the same reference.

3.2. UHECR Bounds – Model 2

Next, obtain Cherenkov bounds [2, 3] for the nine parameters $\vec{\alpha}$ of Model 2. Start with the 15 Auger events [30] of Table 1 on the next page, where the event identification number is given in column 1, the energy E_{prim} of a hadron primary in column 2, the shower-maximum atmospheric depth X_{max} in column 3, and pseudo-random event directions with right ascension $\text{RA}' \in [0, 360^\circ]$ and declination $\text{DEC}' \in [-70^\circ, 25^\circ]$ in column 4.³ These are high-quality events, having been observed in the “hybrid” mode (Fig. 5) of the Pierre Auger Observatory [29]. Specifically, the X_{max} values give information on the primary particle type, as discussed in Ref. [3] and references therein.

As mentioned in Sec. 2.2, vacuum Cherenkov bounds can only be obtained for parameters $\vec{\alpha}$ in domain (18), for which the phase velocity of light is less than the maximal attainable velocity c of the charged particle. Now determine a hypersphere S_a^8 of radius a in this subspace, so that for *each* $\vec{\alpha} \in S_a^8$ the Cherenkov threshold condition (19), with expression (14) inserted, is violated for *at least one* event from Table 1.

The excluded domain of parameter space then corresponds to the region on or outside this hypersphere S_a^8 . Namely, for a positive integrand of the ramp function on the right-hand side of (14), the first term on the right-hand side is multiplied by a factor $1/\lambda$ under scaling of $\vec{\alpha} \rightarrow \lambda \vec{\alpha}$ (and $\varepsilon \rightarrow \lambda \varepsilon$) with $\lambda > 1$, so that inequality (19) is violated for $\lambda > 1$ if it is already for $\lambda = 1$. The events from Table 1 give at the 2σ level:

$$D_{\text{excluded}}^a = D_{\text{causal}}^{(\text{open})} \cap \{\vec{\alpha} \in \mathbb{R}^9 : |\vec{\alpha}| \geq a\}, \quad (22a)$$

$$a \approx 3 \times 10^{-18} \left(\frac{M_{\text{prim}}}{16 \text{ GeV}/c^2} \right)^2, \quad (22b)$$

where $|\vec{\alpha}|$ is the standard Euclidean norm (12) and where the mass of the primary charged particle has conservatively been taken equal to that of oxygen (most primaries in the sample are expected to be protons and helium nuclei).

The resulting UHECR Cherenkov bounds for nonbirefringent modified-Maxwell theory can be described as follows: considering deformation parameters $\alpha^0, \dots, \alpha^8$ with a corresponding phase velocity of light less than the maximal attainable velocity of charged particles, each of these nine parameters must separately have a modulus less than the value a given by (22b). Improving slightly by considering all nine parameters simultaneously, the new 2σ bound from astrophysics is given by

$$\vec{\alpha} \in D_{\text{causal}}^{(\text{open})} : |\vec{\alpha}|^2 \equiv \sum_{l=0}^8 (\alpha^l)^2 < \left(3 \times 10^{-18} \right)^2, \quad (23)$$

with M_{prim} simply set to $16 \text{ GeV}/c^2$.

³ The directions of these 15 events have not yet been released by the Pierre Auger Collaboration and, for this reason, fictional directions have been given in Table 1 (with primes alerting to their nonreality). The bounds of this subsection are based on the numbers given in Table 1, but we are confident that the same bounds are obtained from the actual event directions when they are made available by the Pierre Auger Collaboration. For the bounds obtained here, it only matters that there are 15 UHECR events with more or less equal energies $E_{\text{prim}} \approx 15 \text{ EeV}$ and more or less random directions over a significant part of the sky, the precise association of energy and direction being irrelevant.

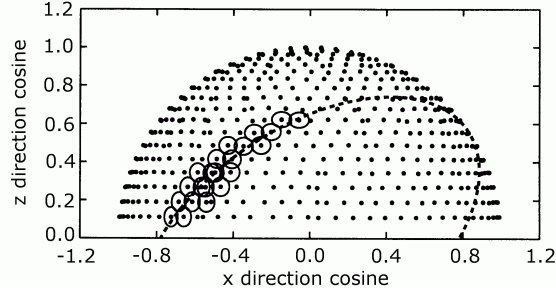


FIGURE 4. Pointing directions of the 22 photomultiplier tubes which triggered in connection with the Fly’s Eye event [26] of October 15, 1991 at 7:34:16 UT. The pointing directions are shown projected into the x - z plane, where the x -axis points east, the y -axis north, and the z -axis upward. The triggered phototubes have positive y -components. The dashed line indicates the plane defined by the shower axis and the detector. See Ref. [26] for further details (figure reproduced by permission of the AAS).

TABLE 1. “Hybrid” events recorded by the Pierre Auger Observatory [29, 30]; see Sec. 3.2 in the main text for further details.

ID No.	E_{prim} [EeV]	X_{max} [g cm^{-2}]	(RA' , DEC') [deg]
668949'	18	765	(356, -29)
673409'	13	760	(344, -62)
828057'	14	805	(086, -34)
986990'	16	810	(152, -33)
1109855'	17	819	(280, -30)
1171225'	16	786	(309, -70)
1175036'	18	780	(228, +17)
1421093'	27	831	(079, +13)
1535139'	16	768	(006, -62)
1539432'	13	787	(153, -15)
1671524'	14	806	(028, -63)
1683620'	21	824	(024, -23)
1687849'	17	780	(031, -23)
2035613'	12	802	(079, -08)
2036381'	29	782	(158, -03)

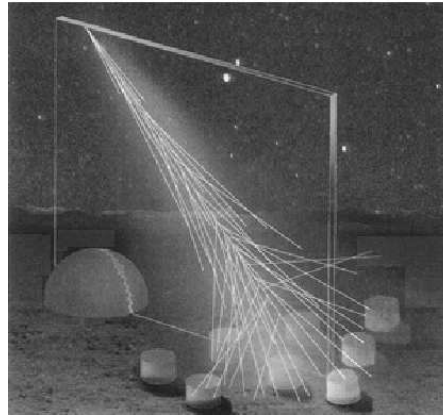


FIGURE 5. The hybrid nature of the Pierre Auger Observatory [29] provides for two independent ways to study extensive air showers, namely, by an array of surface water-Cherenkov detectors and a collection of air-fluorescence telescopes [see <http://www.auger.org/>].

Three remarks are in order. First, bound (23) holds for the reference frame in which the cosmic-ray energies are measured. This frame is essentially given by the rest system of the Sun. Second, the restriction of $\vec{\alpha}$ to domain (18) makes the Cherenkov bound (23) effectively “one-sided,” as discussed in the third paragraph of Sec. 3.1. To specify the precise domain in the 9-dimensional parameter space requires, however, some care. For example, in the 2-dimensional subspace with only $\alpha^0 \equiv \alpha \cos \phi$ and $\alpha^1 \equiv \alpha \sin \phi$ nonzero, the allowed domain from (23) is given by an open disk segment with $-\pi/4 < \phi < \pi/4$ and $0 \leq \alpha < 3 \times 10^{-18}$. Third, consider the restricted *isotropic* model with only parameter α^0 nonzero, which was already discussed in the paragraph containing the exact tree-level results (15)–(17). Then, the *single* Fly’s Eye event [26] with $E_{\text{prim}} \approx 300 \text{ EeV}$ (or the single 200 EeV Auger event [30] mentioned in Sec. 3.1) gives a one-sided bound on α^0 at the 10^{-23} level; see Eq. (C6) of Ref. [2]. This single α^0 bound corresponds, in fact, to the negative part of the previous bound (20a).

At this moment, it may be of interest to recall the best bounds from laboratory experiments [33, 34, 35]:

- for the spatially isotropic nonbirefringent deformation parameter α^0 , there is a direct bound at the 10^{-7} level [33(c)] and an indirect (electron anomalous-magnetic-moment) bound at the 10^{-8} level [34(c)];
- for the eight other nonbirefringent parameters $\alpha^1, \dots, \alpha^8$, there are direct bounds at the 10^{-12} to 10^{-16} levels [35].

Observe that, for Earth-based cavity experiments with an orbital velocity v_{\oplus} around the Sun, the parity-odd parameters α^l , for $l = 1, 2, 3$, typically enter the measured relative frequency shift with a factor $(v_{\oplus}/c) \approx 10^{-4}$, which reduces the sensitivity for these three parameters. In these and other experiments, the parameter α^0 even enters with a quadratic boost factor (precisely which velocity plays a decisive role depends on the experimental setup) and the sensitivity is reduced also for this parameter. See Refs. [15, 33, 35] for further details.

Astrophysics and laboratory bounds on $\vec{\alpha}$ are not directly comparable, the latter having all the benefits of repeatability and control. But the astrophysics bounds at the 10^{-18} level are certainly indicative. Moreover, the UHECR Cherenkov bounds on $\vec{\alpha}$ can be expected to drop to the 10^{-23} level in the coming years [3].

3.3. UHECR Bounds – Implications

In Sec. 3.1, we have obtained Cherenkov bounds for the effective defect excluded-volume factor \tilde{F} and the effective defect size \tilde{b} in the modified photon dispersion relation (3b):

$$0 \leq \tilde{F} \lesssim 10^{-23}, \quad (24a)$$

$$0 \leq \tilde{b} \lesssim 10^{-26} \text{ m} \approx \hbar c / (2 \times 10^{10} \text{ GeV}), \quad (24b)$$

where the last bound follows from (20b) with $\tilde{\sigma}_4 \tilde{F} = 3 \times 10^{-23}$ inserted. But even the “weakened” bound (24b) is already quite remarkable compared to the previous bound (1)

mentioned in the Introduction and, more generally, to what can be achieved with particle accelerators on Earth (the upcoming Large Hadron Collider at CERN will have a proton beam energy $E_p \approx 7 \times 10^3$ GeV). In fact, bound (24b) appears to rule out so-called TeV–gravity models; see Endnote [49] of Ref. [1], which contains further references.

Still, the most interesting bound may very well be (24a), as it rules out a single-scale classical spacetime foam having approximately equal effective defect size \tilde{b} and separation \tilde{l} , with an excluded-volume factor $\tilde{F} \equiv (\tilde{b}/\tilde{l})^4 \sim 1$. Moreover, this conclusion holds for arbitrarily small values of the effective defect size \tilde{b} , as long as a classical spacetime makes sense.

More generally, also the nineteen Lorentz-violating deformation parameters of the modified-Maxwell theory (6) are strongly bounded, as discussed in Sec. 3.2:

$$0 \leq |\kappa^{\mu\nu\rho\sigma}| \lesssim 10^{-18}, \quad (25)$$

where, for the sake of argument, nine “one-sided” Cherenkov bounds from (23) have been made “two-sided” (the even stronger astrophysics bounds [15] on the ten birefringent parameters are already two-sided). A similar bound has been obtained for the stochastic model mentioned a few lines below (11); see, in particular, bound (11b) from Ref. [17(b)].

A priori, one expects $O(1)$ effects for (24a) and (25) if there is some kind of nontrivial small-scale structure of classical spacetime. This expectation is based on an early observation by Veltman [36] that, if a symmetry (for him, gauge invariance) of the quantum field theory considered is violated by the high-energy cutoff Λ (or by a more fundamental theory), then, without fine tuning, the low-energy effective theory may contain symmetry-violating terms which are not suppressed by inverse powers of the cutoff energy Λ . The same observation holds for Lorentz invariance, as emphasized recently by the authors of Ref. [37].

Contrary to these expectations, the experimental bounds (24a) and (25) seem to indicate that Lorentz invariance remains perfectly valid down towards smaller and smaller distances. In fact, this conclusion would appear to hold down to distances at which the classical–quantum transition of spacetime occurs (generally considered to be equal to the so-called Planck length).

In the next section, we will try to make a first step towards understanding the robustness of Lorentz invariance, starting from a physical picture based on a dynamic spacetime and quantum uncertainty (entirely in the spirit of Einstein and Heisenberg). It may be of interest to mention one other possible explanation in the context of so-called “emerging-gravity” models [38, 39, 40, 41], which relies on the existence of a trans-Planckian energy scale in a fundamental Lorentz-violating theory with a topologically protected Fermi point [42]. But this avenue will not be pursued further here.

4. QUANTUM-SPACETIME CONJECTURES

The main conclusion from Sec. 3.3 is that Lorentz invariance appears to remain valid down towards smaller and smaller distances, even down to distances at which the classical–quantum transition of spacetime is believed to occur. That distance is usually

taken to be the Planck length [7, 43, 44],

$$l_{\text{Planck}} \equiv \sqrt{\hbar G/c^3} \approx 1.6 \times 10^{-35} \text{ m} \approx \hbar c / (1.2 \times 10^{19} \text{ GeV}). \quad (26)$$

The question, however, is whether or not quantum spacetime effects show up *only* at distances of the order of the Planck length. Perhaps a quantum spacetime foam [6, 7, 8, 9] could arise primarily from gravitational self-interactions which need not involve Newton’s constant G describing the gravitational coupling of matter (similar to the case of a gas of instantons in Yang–Mills theory).

This brings us to the following suggestion:

Conjecture 1 *Quantum spacetime has a fundamental length scale l which is essentially different from the length l_{Planck} as defined by (26).*

Concretely, this length l could have a different dependence on G than the Planck length. In the next two subsections, we will argue that the standard theory appears to leave some room for a new fundamental constant l and, in the third subsection, we will present a further conjecture as to what physics may be involved.

4.1. Generalized Action

Our starting point is Feynman’s insight [45] that the quantum world of probability amplitudes for matter is governed by the complex phase factor $\exp(i\mathcal{J}_M)$ with a real phase $\mathcal{J}_M = S_M/\hbar$ expressed in terms of the classical matter action S_M and the reduced Planck constant $\hbar \equiv h/2\pi$.

As the merging of quantum mechanics and gravitation is far from understood, it may be sensible to consider a *generalized* dimensionless action for “quantum gravity” (or, better, “quantum spacetime”) as probed by classical matter:

$$\mathcal{J}_{\text{grav}} = \frac{-1}{16\pi l^2} \int d^4x \sqrt{|g(x)|} (R(x) + 2\lambda) + \frac{G/c^3}{l^2} \int d^4x \sqrt{|g(x)|} \mathcal{L}_M^{\text{class}}(x), \quad (27)$$

with the Ricci curvature scalar $R(x)$, a new fundamental length scale l , and a nonnegative cosmological constant $\lambda \geq 0$.

Two remarks may be helpful. First, expression (27) is to be used only for a rough description of possible quantum effects of spacetime, not for those of the matter fields which are considered to act as a classical source with coupling constant G . Second, the special case $l^2 = l_{\text{Planck}}^2$ reduces the dimensionless action (27) to the standard expression [9], with the Einstein–Hilbert integral multiplied by the factor $-c^3/(16\pi G)$ and the matter integral by $1/\hbar$. Here, however, we wish to explore the possibility that l is an entirely new length scale independent of l_{Planck} (Conjecture 1).

The overall factor l^{-2} in (27) is irrelevant for obtaining the classical field equations,

$$R^{\mu\nu}(x) - \frac{1}{2} g^{\mu\nu}(x) R(x) - \lambda g^{\mu\nu}(x) = -8\pi G T_M^{\mu\nu}(x), \quad (28)$$

where the matter energy-momentum tensor $T_M^{\mu\nu}(x)$ is defined by an appropriate functional derivative of $\int d^4x \sqrt{|g|} \mathcal{L}_M^{\text{class}}$. But, following Feynman, the physics of a genuine

quantum spacetime would be governed by the complex phase factor $\exp(i\mathcal{I}_{\text{grav}})$ and the overall factor of l^{-2} in (27) would be physically relevant. Just to be clear, we do not claim that a future theory of quantum gravity must necessarily be formulated as a path integral but only wish to use the Feynman phase factor as a heuristic device in order to say something about the typical length scale involved.

The expression (27) for the generalized quantum phase also suggests that, as far as spacetime is concerned, the role of Planck’s constant \hbar would be replaced by the squared length l^2 , which might loosely be called the “quantum of area” (see, e.g., Ref. [46] for a calculation in the context of loop quantum gravity and Refs. [47, 48] for general remarks on a possible minimum length). Planck’s constant \hbar would continue to play a role in the description of the matter quantum fields.

However, with \hbar and l^2 being logically independent, it is possible to consider the “limit” $\hbar \rightarrow 0$ (matter behaving classically) while keeping l^2 fixed (spacetime behaving nonclassically). Even if the numerical values of the lengths l and l_{Planck} will turn out to be close (or equal) in the end, it may be conceptually interesting to consider phases of the theory with ratios l/l_{Planck} very different from unity.

4.2. Fundamental Constants

The fundamental dimensionful constants encountered in the previous subsection are summarized in Table 2 on the next page. In this contribution, we mainly consider the second and third columns of Table 2 (removing the parentheses around G) and leave the rigorous treatment of *all* columns to a future theory. In this subsection, however, we already make some speculative remarks on a possible new theory encompassing all of the physics arenas appearing in Table 2.

In that future theory, “classical gravitation” may perhaps be induced [49] by *combined* quantum effects of matter and spacetime, giving Newton’s gravitational constant

$$G = \zeta c^3 l^2 / \hbar, \quad (29)$$

with a calculable numerical coefficient $\zeta \geq 0$.⁴ In this way, the “large” classical coupling constant G would be the ratio of “small” quantum constants l^2 and \hbar . Practically, the numerical coefficient ζ gives the ratio l_{Planck}^2/l^2 .

The dimensionful constants \hbar , c , and l^2 of Table 2 correspond to, respectively, the quantum of action, the limiting speed of a massive particle, and the quantum of area (up to an as yet undetermined numerical factor). In addition, each of these constants is believed to play “the role of a conversion factor that is essential to implementing a profound physical concept” (quoting from Ref. [44]).

The role of the individual constants c and \hbar is clear: the first converts time into length according to relativity theory ($cT = L$, where physical quantities to be converted are denoted by capital letters) and the second converts frequency or inverse time into energy

⁴ There may or may not be a connection with the “emergent-gravity” models mentioned in the last paragraph of Sec. 3.3. See also Ref. [50] for an interesting comparison to hydrodynamics.

TABLE 2. Fundamental dimensionful constants of nature, including the hypothetical quantum of area l^2 . The gravitational constant G appears between brackets, as it can, in principle, be expressed in terms of the other constants; see (29) in the main text.

quantum matter	classical relativity	quantum spacetime
\hbar	c (G)	l^2

according to quantum theory ($\hbar \Omega = \hbar 2\pi/T = E$). From Einstein’s theory of gravity and relation (29), it would seem that the combination $l^2/(\hbar c)$ acts as the conversion factor between space curvature (with dimensions of inverse length square) and energy density (with dimensions of energy over length cube), so that $1/L^2 \sim \zeta l^2/(\hbar c) E/L^3$, with the numerical coefficient ζ from (29). Replacing the energy E by Mc^2 , these conversion factors are summarized in Fig. 6. Starting with LENGTH on the left of this figure and going around clockwise, the required number of fundamental constants is seen to accumulate steadily.

In the previous paragraph, we have found the conversion factor between mass and length by relying on Einstein’s theory of gravity. Incidentally, the simplest way to get this conversion factor may be to use the standard result for the Schwarzschild radius of a central mass M , $R_{\text{Schw}} \equiv 2GM/c^2$, and to replace G therein by (29). For the corresponding arrow in Fig. 6, this would imply that the conversion factor $l^2 c/\hbar$ comes together with the pure number ζ appearing in (29). However, it might be interesting, as discussed in the last paragraph of Sec. 4.1, to consider a possible phase of the theory with $\zeta = 0$ and still keep the linear relation between mass and length.

For $\zeta = 0$, the physical interpretation of the conversion factor $l^2 c/\hbar$ in Fig. 6 is entirely open (hence, the dotted arrow in the figure). A trivial suggestion (definitely not yet a “profound physical concept”) would run as follows. Given the fundamental length scale l and the constants c and \hbar , a corresponding energy density is defined as $\tilde{\rho} \equiv \hbar c/l^4$. Then, one possible physical interpretation would be that the mass M of an “elementary particle” is associated to a characteristic length \tilde{L} in such a way that the fundamental energy density $\tilde{\rho}$ over a volume \tilde{V} obtained by multiplying \tilde{L} with the minimum area l^2 ,

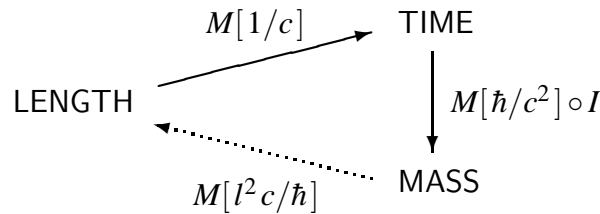


FIGURE 6. Fundamental dimensionful constants \hbar , c , and l^2 from Table 2 in the role of conversion factors, with numerical coefficients omitted. The operation $M[z]$ stands for multiplication by z and the operation I for inversion. Hence, time is first inverted (to give a frequency) and then multiplied by \hbar/c^2 (to give a mass). The linear relation between mass and length is discussed in Sec. 4.2 of the main text.

$\tilde{V} \equiv \tilde{L} l^2$, returns the original mass, $M \equiv \tilde{V} \tilde{\rho}$. In this way, the associated length \tilde{L} of a mass M would correspond to the largest linear spread a fiducial volume $V \equiv M/\tilde{\rho}$ could have, provided the area of any cross section of the volume V is not allowed to drop under the value l^2 . The heuristic idea behind this length \tilde{L} is that an inserted material mass M distorts the intrinsic foam-like structure of space.

Observe that the mass dependence of the associated length $\tilde{L} \equiv M l^2 c/\hbar$ is opposite to that of the standard Compton (reduced) wavelength $\tilde{\lambda}_C \equiv \hbar/(Mc)$. For the known elementary particles, with M of the order of $10^2 \text{ GeV}/c^2$ or less, and l below the value quoted in (24b), the mass-induced fuzziness scale \tilde{L} of a particle will be very much smaller than the corresponding Compton wavelength $\tilde{\lambda}_C$. Specifically, the ratio of these two length scales is given by the inverse ratio of the corresponding squared energies, $\tilde{L}/\tilde{\lambda}_C = (Mc^2/(\hbar c/l))^2$.

At this moment, it may be helpful to list all the length scales possibly relevant to an elementary particle with mass M (in order of increasing size, taking $\zeta < 1/2$ and temporarily setting $c = \hbar = 1$): the Schwarzschild radius $R_{\text{Schw}} \equiv 2\zeta l^2 M$, the mass-induced fuzziness scale $\tilde{L} \equiv l^2 M$, the fundamental quantum-spacetime length scale l , and the Compton wavelength $\tilde{\lambda}_C \equiv 1/M$. In principle, the mass-induced fuzziness scale \tilde{L} (or perhaps even the larger intrinsic fuzziness scale l) could lead to form-factor effects in high-energy scattering processes and possibly affect the renormalization of the standard-model quantum field theory. A minimum length may even play a crucial role in obtaining the usual rules of quantum mechanics, as discussed in Ref. [51].

4.3. Vacuum Energy Density

Let us return to the generalized action (27), with Newton's gravitational constant G appearing explicitly but without Planck's constant \hbar . If Conjecture 1 holds true, the question arises as to what type of physics determines the length scale l . Here, we assume this physics to be independent of \hbar , otherwise the discussion would be more along the lines sketched in the previous subsection. One possible answer would then be given by the following suggestion:

Conjecture 2 *The quantum-spacetime length scale l is related to a nonvanishing cosmological constant or vacuum energy density.*

For the case of the early universe, with a vacuum energy density $\rho_{\text{vac}} \equiv E_{\text{vac}}^4/(\hbar c)^3$ in the matter part of the action (27) and $\lambda = 0$ in the geometric part, it can be argued [4] that the following approximate relation holds (\hbar appears only as an auxiliary constant):

$$l \stackrel{?}{\sim} c^2/\sqrt{G\rho_{\text{vac}}} = \hbar c E_{\text{Planck}}/E_{\text{vac}}^2 \approx 2 \times 10^{-29} \text{ m} \left(\frac{E_{\text{Planck}}}{10^{19} \text{ GeV}} \right) \left(\frac{10^{16} \text{ GeV}}{E_{\text{vac}}} \right)^2, \quad (30)$$

where the Planck energy scale is given by $E_{\text{Planck}} \equiv \hbar c/l_{\text{Planck}}$ and the numerical value for E_{vac} has been identified with the “grand-unification” scale suggested by elementary particle physics [5, 52]. As anticipated in the sentence under Conjecture 1, the length scale l as given by the first mathematical expression on the right-hand side of (30) has a G dependence which is different from that of the standard Planck length (26).

If (30) holds true with $l_{\text{Planck}}/l \sim 10^{-6}$, it is perhaps possible to have *sufficiently rare* defects left over from the crystallization process of an initial quantum spacetime foam to a classical spacetime.⁵ With the effective defect size \tilde{b} set by l_{Planck} (matter related) and the effective defect separation \tilde{l} set by l (vacuum related), these spacetime defects would give the following excluded-volume factor in the modified photon dispersion relation (3b):

$$\tilde{F} \equiv (\tilde{b}/\tilde{l})^4 \stackrel{?}{\sim} 10^{-24}, \quad (31)$$

which is close to saturating the current UHECR bound (20a). As mentioned at the end of Sec. 3.1, a possible detection of Lorentz-violating effects (having ruled out conventional explanations) would be an entirely different matter than setting better and better bounds on the small-scale structure of spacetime, even though the latter type of “null experiments” can also be of great importance (think of the role of the Michelson–Morley experiment for the discovery of special relativity [54]).

5. SUMMARY

The main phenomenological conclusion of the first part of this review (Secs. 2 and 3) is that quantum spacetime foam, if at all real, appears to have given rise to a classical spacetime manifold which is remarkably smooth. Using astrophysics data, this result can be quantified as follows: the defect excluded-volume factor in the modified proton and photon dispersion relations (3ab) is bounded by $\tilde{F} \lesssim 10^{-23} \ll 1$ and the Lorentz-violating parameters in the modified-Maxwell theory (6) by $|\kappa^{\mu\nu\rho\sigma}| \lesssim 10^{-18} \ll 1$.

Prompted by this phenomenological conclusion, a theoretical suggestion has been advanced in the second part (Sec. 4), namely, that the quantum theory of spacetime may have a fundamental length scale l conceptually different from the Planck length (Conjecture 1) and possibly related to vacuum energy density (Conjecture 2). With two length scales present, l and l_{Planck} , it is perhaps possible to satisfy the tight experimental constraint on \tilde{F} .

Still, it is safe to say that the quantum origin of classical spacetime remains a mystery.

ACKNOWLEDGMENTS

It is a pleasure to thank the organizers for bringing about this interesting “Symposium on Gravitation and Cosmology” (El Colegio Nacional, Mexico City, September 2007) and the participants for informative discussions. The participants of another meeting, “Condensed Matter Meets Gravity” (Lorentz Center, Leiden, August 2007), are also thanked for equally informative discussions.

⁵ It is likely that a proper understanding of this crystallization process requires new ideas about the quantum measurement problem and possibly even a mechanism for objective state reduction [53].

REFERENCES

1. S. Bernadotte and F.R. Klinkhamer, “Bounds on length scales of classical spacetime foam models,” *Phys. Rev. D* **75**, 024028 (2007), arXiv:hep-ph/0610216.
2. C. Kaufhold and F.R. Klinkhamer, “Vacuum Cherenkov radiation in spacelike Maxwell–Chern–Simons theory,” *Phys. Rev. D* **76**, 025024 (2007), arXiv:0704.3255 [hep-th].
3. F.R. Klinkhamer and M. Risse, “Ultrahigh-energy cosmic-ray bounds on nonbirefringent modified-Maxwell theory,” to appear in *Phys. Rev. D*, arXiv:0709.2502 [hep-ph].
4. F.R. Klinkhamer, “Fundamental length scale of quantum spacetime foam,” *JETP Lett.* **86**, 73 (2007), arXiv:gr-qc/0703009.
5. C. Itzykson and J.-B. Zuber, *Quantum Field Theory*, McGraw–Hill, New York, 1980.
6. J.A. Wheeler, “On the nature of quantum geometrodynamics,” *Ann. Phys. (N.Y.)* **2**, 604 (1957).
7. J.A. Wheeler, “Superspace and the nature of quantum geometrodynamics,” in *Battelle Rencontres 1967*, edited by C.M. DeWitt and J.A. Wheeler, Benjamin, New York, 1968, pp. 242–307.
8. S.W. Hawking, “Space-time foam,” *Nucl. Phys. B* **144**, 349 (1978).
9. M. Visser, *Lorentzian Wormholes: From Einstein to Hawking*, Springer, New York, 1996.
10. H.A. Bethe, “Theory of diffraction by small holes,” *Phys. Rev.* **66**, 163 (1944).
11. R. Lehnert, “Threshold analyses and Lorentz violation,” *Phys. Rev. D* **68**, 085003 (2003), arXiv:gr-qc/0304013.
12. C. Kaufhold and F.R. Klinkhamer, “Vacuum Cherenkov radiation and photon triple-splitting in a Lorentz-noninvariant extension of quantum electrodynamics,” *Nucl. Phys. B* **734**, 1 (2006), arXiv:hep-th/0508074.
13. S. Chadha and H.B. Nielsen, “Lorentz invariance as a low-energy phenomenon,” *Nucl. Phys. B* **217**, 125 (1983).
14. D. Colladay and V.A. Kostelecký, “Lorentz-violating extension of the standard model,” *Phys. Rev. D* **58**, 116002 (1998), arXiv:hep-ph/9809521.
15. V.A. Kostelecký and M. Mewes, “Signals for Lorentz violation in electrodynamics,” *Phys. Rev. D* **66**, 056005 (2002), arXiv:hep-ph/0205211.
16. Q.G. Bailey and V.A. Kostelecký, “Lorentz-violating electrostatics and magnetostatics,” *Phys. Rev. D* **70**, 076006 (2004), arXiv:hep-ph/0407252.
17. (a) F.R. Klinkhamer and C. Rupp, “Spacetime foam, CPT anomaly, and photon propagation,” *Phys. Rev. D* **70**, 045020 (2004), arXiv:hep-th/0312032; (b) F.R. Klinkhamer and C. Rupp, “Photon-propagation model with random background field: Length scales and Cherenkov limits,” *Phys. Rev. D* **72**, 017901 (2005), arXiv:hep-ph/0506071.
18. B.L. Hu and K. Shiokawa, “Wave propagation in stochastic spacetimes: Localization, amplification and particle creation,” *Phys. Rev. D* **57**, 3474 (1998), arXiv:gr-qc/9708023.
19. B. Altschul, “Vacuum Čerenkov radiation in Lorentz-violating theories without CPT violation,” *Phys. Rev. Lett.* **98**, 041603 (2007), arXiv:hep-th/0609030.
20. C. Kaufhold, F.R. Klinkhamer, and M. Schreck, “Tree-level calculation of vacuum Cherenkov radiation in isotropic nonbirefringent modified-Maxwell theory,” report KA–TP–32–2007.
21. C. Adam and F.R. Klinkhamer, “Causality and CPT violation from an Abelian Chern–Simons-like term,” *Nucl. Phys. B* **607**, 247 (2001), arXiv:hep-ph/0101087.
22. V.A. Kostelecký and R. Lehnert, “Stability, causality, and Lorentz and CPT violation,” *Phys. Rev. D* **63**, 065008 (2001), arXiv:hep-th/0012060.
23. J. Bros and H. Epstein, “Microcausality and energy positivity in all frames imply Lorentz invariance of dispersion laws,” *Phys. Rev. D* **65**, 085023 (2002), arXiv:hep-th/0204118.
24. E.F. Beall, “Measuring the gravitational interaction of elementary particles,” *Phys. Rev. D* **1**, 961 (1970), Sec. III A.
25. S.R. Coleman and S.L. Glashow, “Cosmic ray and neutrino tests of special relativity,” *Phys. Lett. B* **405**, 249 (1997), arXiv:hep-ph/9703240.
26. D.J. Bird et al., “Detection of a cosmic ray with measured energy well beyond the expected spectral cutoff due to cosmic microwave radiation,” *Astrophys. J.* **441**, 144 (1995), arXiv:astro-ph/9410067.
27. O. Gagnon and G.D. Moore, “Limits on Lorentz violation from the highest energy cosmic rays,” *Phys. Rev. D* **70**, 065002 (2004), arXiv:hep-ph/0404196.
28. F.R. Klinkhamer and C. Rupp, “Spacetime foam and high-energy photons,” to appear in *New. Astron. Rev.*, arXiv:astro-ph/0511267.

29. J. Abraham et al. [Pierre Auger Collaboration], “Properties and performance of the prototype instrument for the Pierre Auger Observatory,” *Nucl. Instrum. Meth.* A523, 50 (2004).
30. J. Abraham et al. [Pierre Auger Collaboration], “An upper limit to the photon fraction in cosmic rays above 10^{19} eV from the Pierre Auger Observatory,” *Astropart. Phys.* 27, 155 (2007), arXiv:astro-ph/0606619.
31. J. Albert et al. [MAGIC Collaboration], “Probing quantum gravity using photons from a Mkn 501 flare observed by MAGIC,” arXiv:0708.2889v1 [astro-ph].
32. J. Albert et al. [MAGIC Collaboration], “Variable VHE gamma-ray emission from Markarian 501,” arXiv:astro-ph/0702008v2.
33. (a) G. Saathoff et al., “Improved test of time dilation in special relativity,” *Phys. Rev. Lett.* 91, 190403 (2003); (b) M.E. Tobar, P. Wolf, A. Fowler, and J.G. Hartnett, “New methods of testing Lorentz violation in electrodynamics,” *Phys. Rev. D* 71, 025004 (2005), arXiv:hep-ph/0408006; (c) M. Hohensee et al., “Erratum: New methods of testing Lorentz violation in electrodynamics,” *Phys. Rev. D* 75, 049902(E) (2007), arXiv:hep-ph/0701252.
34. (a) B. Odom, D. Hanneke, B. D’Urso, and G. Gabrielse, “New measurement of the electron magnetic moment using a one-electron quantum cyclotron,” *Phys. Rev. Lett.* 97, 030801 (2006); (b) G. Gabrielse, D. Hanneke, T. Kinoshita, M. Nio, and B. Odom, “New determination of the fine structure constant from the electron g value and QED,” *Phys. Rev. Lett.* 97, 030802 (2006); 99, 039902(E) (2007); (c) C.D. Carone, M. Sher, and M. Vanderhaeghen, “New bounds on isotropic Lorentz violation,” *Phys. Rev. D* 74, 077901 (2006), arXiv:hep-ph/0609150.
35. (a) P.L. Stanwix et al., “Improved test of Lorentz invariance in electrodynamics using rotating cryogenic sapphire oscillators,” *Phys. Rev. D* 74, 081101 (2006), arXiv:gr-qc/0609072; (b) H. Müller et al., “Relativity tests by complementary rotating Michelson-Morley experiments,” *Phys. Rev. Lett.* 99, 050401 (2007), arXiv:0706.2031 [physics.class-ph].
36. M. Veltman, “The infrared–ultraviolet connection,” *Acta Phys. Polon.* B12, 437 (1981).
37. J. Collins, A. Perez, D. Sudarsky, L. Urrutia, and H. Vucetich, “Lorentz invariance: An additional fine-tuning problem,” *Phys. Rev. Lett.* 93, 191301 (2004), arXiv:gr-qc/0403053.
38. J.D. Bjorken, “Emergent gauge bosons,” arXiv:hep-th/0111196.
39. R.B. Laughlin, “Emergent relativity,” *Int. J. Mod. Phys. A* 18, 831 (2003), arXiv:gr-qc/0302028.
40. C.D. Froggatt and H.B. Nielsen, “Derivation of Poincaré invariance from general quantum field theory,” *Ann. Phys. (Leipzig)* 14, 115 (2005), arXiv:hep-th/0501149.
41. G.E. Volovik, “Fermi-point scenario for emergent gravity,” arXiv:0709.1258 [gr-qc].
42. F.R. Klinkhamer and G.E. Volovik, “Merging gauge coupling constants without grand unification,” *JETP Lett.* 81, 551 (2005), arXiv:hep-ph/0505033.
43. M. Planck, “Über irreversibele Strahlungsvorgänge,” *Sitzungsber. Preuss. Akad. Wiss. Berlin, Math. Phys. Klasse*, pp. 440–480 (1899), Sec. 26.
44. F. Wilczek, “On absolute units. I: Choices,” *Phys. Today* 58N10, 12 (2005).
45. R.P. Feynman, “Space-time approach to nonrelativistic quantum mechanics,” *Rev. Mod. Phys.* 20, 367 (1948).
46. C. Rovelli and L. Smolin, “Discreteness of area and volume in quantum gravity,” *Nucl. Phys.* B442, 593 (1995); B456, 753(E) (1995), arXiv:gr-qc/9411005.
47. C.A. Mead, “Possible connection between gravitation and fundamental length,” *Phys. Rev.* 135, B849 (1964); “Observable consequences of fundamental-length hypotheses,” *Phys. Rev.* 143, 990 (1966).
48. L.J. Garay, “Quantum gravity and minimum length,” *Int. J. Mod. Phys. A* 10, 145 (1995), arXiv:gr-qc/9403008.
49. (a) A.D. Sakharov, “Vacuum quantum fluctuations in curved space and the theory of gravitation,” *Sov. Phys. Dokl.* 12, 1040 (1968), reprinted in *Gen. Rel. Grav.* 32, 365 (2000); (b) M. Visser, “Sakharov’s induced gravity: A modern perspective,” *Mod. Phys. Lett. A* 17, 977 (2002), arXiv:gr-qc/0204062.
50. G.E. Volovik, “From quantum hydrodynamics to quantum gravity,” arXiv:gr-qc/0612134.
51. R.V. Buniy, S.D.H. Hsu, and A. Zee, “Discreteness and the origin of probability in quantum mechanics,” *Phys. Lett. B* 640, 219 (2006), arXiv:hep-th/0606062.
52. H. Georgi, H.R. Quinn, and S. Weinberg, “Hierarchy of interactions in unified gauge theories,” *Phys. Rev. Lett.* 33, 451 (1974).
53. R. Penrose, *The Road to Reality*, Knopf, New York, 2005, Sec. 30.14.
54. A. Pais, ‘*Subtle is the Lord . . .*’ *The Science and the Life of Alfred Einstein*, Clarendon Press, Oxford, 1982, Chap. 6.